Cochaperones enable Hsp70 to fold proteins like a Maxwell's demon

Huafeng Xu[1,†]

1 Unaffiliated, Forest Hills, NY 11375, USA.

† Correspondence: huafeng@gmail.com, +1 917 968 8176

Short Title: Hsp70 is a Maxwell's demon

1 Abstract

2 The heat shock protein 70 (Hsp70) chaperones, vital to the proper folding of proteins inside cells,
3 consume ATP and require cochaperones in assisting protein folding. It is unclear whether Hsp70
4 can utilize the free energy from ATP hydrolysis to fold a protein into a native state that is
5 thermodynamically unstable in the chaperone-free equilibrium. Here we present a model of
6 Hsp70-mediated protein folding, which predicts that Hsp70, as a result of differential stimulation
7 of ATP hydrolysis by its Hsp40 cochaperone, dissociates faster from a substrate in fold-
8 competent conformations than from one in misfolding-prone conformations, thus elevating the
9 native concentration above and suppressing the misfolded concentration below their respective
10 equilibrium values. Previous models would not make or imply these predictions, which are
11 experimentally testable. Our model quantitatively reproduces experimental refolding kinetics,
12 predicts how modulations of the Hsp70/Hsp40 chaperone system affect protein folding, and
13 suggests new approaches to regulating cellular protein quality.

14 Keywords: chaperones, Hsp70, Hsp40, protein folding, nonequilibrium thermodynamics

15 Introduction

16 The discovery of chaperones and their roles in assisting protein folding amended the long-held
17 view that proteins spontaneously fold into their native structures[1–3]. Large, multi-domain
18 proteins may take many hours to fold, or fail to fold properly altogether on their own[2,4]. ATP-
19 consuming chaperones—including Hsp70s—provide critical assistance in the in vivo folding and
20 the biological functions of broad sets of substrate proteins[3]. Extensive experimental studies have
21 firmly established that the Hsp70 chaperones can greatly accelerate the folding of their substrate
22 proteins[5,6]. Despite tremendous progress in the mechanistic studies of the Hsp70 chaperones[2,7],
23 including the development of theoretical models[8–10], it remains unclear why ATP consumption is
24 indispensable to these chaperones; enzymes do not need to consume free energy in catalyzing
25 chemical reactions. Recently it was demonstrated that chaperones such as GroEL and Hsp70
26 depend on continuous ATP hydrolysis to maintain a protein in a native state that is
27 thermodynamically unstable[11], but it is unknown how Hsp70 can utilize the ATP free energy to

1

28 alter the folding equilibrium. In addition, Hsp70s require Hsp40—also known as J proteins[12]—
29 cochaperones in assisting protein folding. It is yet unexplained why cochaperones are absolutely
30 necessary.

31 The Hsp70 chaperones, such as the bacterial DnaK, consist of an N-terminal nucleotide binding
32 domain (NBD) and a C-terminal substrate binding domain (SBD). The Hsp70 SBD adopts an
33 open conformation when its NBD is ATP-bound (we call the Hsp70 to be in the ATP-state),
34 which allows the substrate to bind and unbind at high rates, whereas when the NBD is ADP-
35 bound (ADP-state), the SBD changes to a closed conformation, rendering both binding and
36 unbinding orders-of-magnitude slower[6,13,14]. Hsp70s have low basal ATP hydrolysis activities[15].
37 The Hsp40 cochaperones, such as the bacterial DnaJ, can drastically stimulate the ATPase
38 activity of Hsp70 using their N-terminal J domain (JD)[16,17], shared by all Hsp40s (hence the
39 name J proteins)[12]. Hsp40s also have a C-terminal domain (CTD) that can bind to denatured
40 proteins[18,19]. Both Hsp70 and Hsp40 recognize exposed hydrophobic sites[7,20,21]. As a result,
41 they can distinguish different protein conformations using the corresponding difference in the
42 exposed hydrophobic sites. For example, Hsp70 has been shown to bind to both unfolded and
43 partially folded, near native protein structures, but not to native structures[22,23]. Hsp40 and Hsp70
44 may simultaneously bind to different segments of the same substrate molecule, and the
45 consequent spatial proximity then facilitates the J domain binding to Hsp70 and accelerating its
46 ATP hydrolysis[24–26]. Following ATP hydrolysis, the chaperone returns from the ADP-state to
47 the ATP-state through nucleotide exchange, which is often catalyzed by nucleotide exchange
48 factors (NEF) such as the bacterial GrpE[27,28].

49 A protein may fold to its native state, N, or go into a misfolded/aggregated—we will use these
50 two terms interchangeably—state, M (Fig. 1a). It is unknown whether Hsp70 can use the free
51 energy from ATP hydrolysis to drive its substrate toward the native state such that
52 $f_N / f_M > f_{N,eq} / f_{M,eq}$, where f_S is the fraction of the substrate in state S at the steady state of
53 Hsp70-mediated folding, and $f_{S,eq}$ is the corresponding fraction at the folding equilibrium in the
54 absence of the chaperone. Previous models[9,29] mostly considered the chaperone as an
55 unfoldase/holdase—which need not consume free energy—that pulls the substrate out of the
56 misfolded state and holds it in an unfolded state. It was proposed that the free energy from ATP
57 hydrolysis was used to achieve ultra-affinity in substrate binding[8,30]. As an unfoldase/holdase,
58 Hsp70 would also pull the substrate out of the native state into the unfolded state; unless Hsp70
59 has a higher affinity for the native substrate than for the misfolded substrate, these models would
60 predict $f_N / f_M \leq f_{N,eq} / f_{M,eq}$.

61 Here we propose a model of Hsp70-mediated protein folding, in which Hsp70 and Hsp40
62 together constitute a molecular machine that uses the free energy from ATP hydrolysis to
63 actively drive a protein toward its native state, so that $f_N / f_M > f_{N,eq} / f_{M,eq}$. It suggests that
64 without Hsp40, Hsp70 alone cannot change the ratio f_N / f_M from the equilibrium value
65 $f_{N,eq} / f_{M,eq}$. Our model thus answers the question why Hsp70 requires both the Hsp40
66 cochaperones and ATP consumption in assisting protein folding. Our model explains the
67 puzzling non-monotonic dependency of folding efficiency on the chaperone and cochaperone
68 concentrations. It makes quantitative predictions on how protein folding is affected by
69 modulations of the chaperone environment, including changes in the ATPase activity or the
70 nucleotide exchange rate of Hsp70. These predictions may be readily tested by experiments, and
71 inform rational approaches to manipulating chaperone-mediated protein folding.
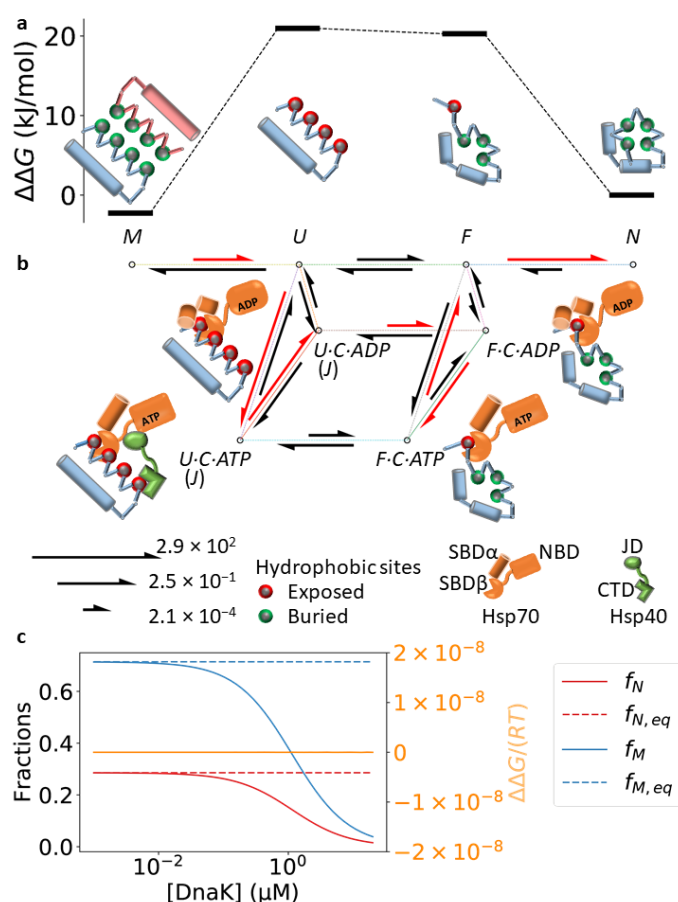
Figure 1. Our model of Hsp70/Hsp40/NEF-mediated protein folding. **a** Conformational states in protein folding, and their relative free energies in the absence of chaperones. We assume that there are four conformational states: *M*isfolded/aggregated, *U*nfolded and aggregation-prone, *F*old-competent, and *N*ative. The pink and blue chains in the *M* state may correspond to different molecules (aggregated) or to different domains in the same molecule (misfolded). The high free energy barriers associated with the intermediate states *U* and *F* slow down the refolding of misfolded proteins. The exemplary free energies are derived from the kinetic parameters fit to the refolding experiments of luciferase at 25 °C (Table 2). **b** The transitions between the microscopic states in the chaperone-mediated folding pathway. $S \cdot C \cdot X$ represents the complex between the substrate in the conformational state S ($= U, F$) and the Hsp70 chaperone (denoted as C) bound to nucleotide X ($= ATP, ADP$). The transitions between S and $S \cdot C \cdot X$ correspond to the chaperone binding to and unbinding from the substrate. The transition of $S \cdot C \cdot ATP$ to $S \cdot C \cdot ADP$ corresponds to ATP hydrolysis, and its reverse, nucleotide exchange. Hsp70 binding stabilizes the substrate in the intermediate states, thus catalyzing the folding reaction. Hsp40 (J) can form a ternary complex with the substrate and Hsp70—thus stimulating ATP hydrolysis—if the substrate is in the U state, but not if the substrate is in the F state. Differential ATP hydrolysis by Hsp70 bound to the substrate in the U and F states drives the refolding through the pathway highlighted in red. The lengths of the reaction arrows are linear with respect to the logarithms of the exemplary rate constants (in 1/s) for the DnaK/DnaJ/GrpE-mediated refolding of luciferase at 25 °C (Table 1, 2). **c** Without cochaperones, Hsp70 cannot alter the balance between folding and misfolding. DnaK binding to the intermediate states decreases both the native (red) and misfolded (blue) populations, but the ratio between the two remains unchanged from its equilibrium value: $\Delta\Delta G = 0$ (orange, right y-axis). Here, we have taken $k_{a,C \cdot ATP}^{(U)}/k_{a,C \cdot ATP}^{(F)} = k_{a,C \cdot ADP}^{(U)}/k_{a,C \cdot ADP}^{(F)} = 100$ to show that differential binding of Hsp70 to the substrate in different conformational states does not alter the folding/misfolding balance.

3

72 Results

73 In our model (detailed in *Methods*), we consider two additional conformational states—besides
74 the *M* and *N* states—of a protein: the unfolded and aggregation-prone state, *U*, and the fold-
75 competent state, *F*. A protein in the *F* state is unfolded but poised to fold into the native state
76 (Fig. 1a, b). Such intermediate states of folding have been observed experimentally[4].
77 Conformational transitions can occur between *M* and *U*, between *U* and *F*, and between *F* and *N*
78 (Fig. 1b). We assume that a protein in the *U* state has more exposed hydrophobic sites than in
79 the *F* state—which is consistent with the experimental observations[4]—and a protein in the *M* and
80 *N* states has nearly zero such sites, as both folding and aggregation (including oligomerization)
81 bury the protein's hydrophobic sites (Fig. 1a).

82 Key to our model is the assumption that Hsp40, like Hsp70, has different affinities for the
83 substrate in different conformations[20], favoring conformations with more exposed hydrophobic
84 sites. Thus Hsp70 and Hsp40 can bind to a substrate molecule in the *U* and *F* states—with
85 higher affinities for the *U* state than for the *F* state—but not to one in the *M* and *N* states
86 (Fig. 1b). A substrate in the *U* state is more likely to be Hsp40-bound than one in the *F* state. As
87 a result, an Hsp70 molecule bound to a substrate molecule in the *U* state will on average have
88 substantially higher ATP hydrolysis rate—because of the more probable *cis* stimulation by an
89 Hsp40 molecule bound to the same substrate molecule—than if it is bound to a substrate
90 molecule in the *F* state. If the nucleotide exchange rate is between these two hydrolysis rates, an
91 Hsp70 bound to a substrate in the *U* state will be driven toward the ADP-state, where it slowly
92 dissociates from the substrate, while an Hsp70 bound to a substrate in the *F* state will be driven
93 toward the ATP-state, where it rapidly dissociates from the substrate. Acting like a Maxwell's
94 demon[31], Hsp70 releases the fold-competent substrate but retains the aggregation-prone
95 substrate, driving the folding along the reaction path of $M \rightarrow U \rightarrow U \cdot C \cdot ATP \rightarrow U \cdot C \cdot ADP$
96 $\rightarrow F \cdot C \cdot ADP \rightarrow F \cdot C \cdot ATP \rightarrow F \rightarrow N$ ($S \cdot C \cdot X$ represents the complex between a substrate in
97 conformation *S* and the chaperone *C* bound to nucleotide $X = ATP, ADP$) (Fig. 1b). One ATP
98 molecule is consumed in this reaction path and the free energy is used to compel the substrate
99 into the native state.

100 The extent to which Hsp70 biases protein folding can be quantified by the excess free energy:
101 $\Delta\Delta G \equiv R\,T\,(\ln(f_N / f_M) - \ln(f_{N,eq} / f_{M,eq}))$, where *R* is the gas constant and *T* the temperature. A
102 positive excess free energy requires not that more chaperones bind to the substrate in the *U* state
103 than to the substrate in the *F* state, which is true and reflected in previous models, but that an
104 individual chaperone molecule, when bound to a substrate, resides longer on it if the substrate is
105 in the *U* state than if it is in the *F* state. For this, Hsp70 needs both ATP consumption and a
106 cochaperone: it can be shown algebraically (see *Methods*) and numerically (Fig. 1c) that without
107 cochaperones, $\Delta\Delta G = 0$. These predictions are consistent with the results from the single-
108 molecule experiment of DnaK-mediated refolding[32], where DnaK alone in the presence of ATP
109 was unable to alter the ratio of the misfolded and folded fractions.

110 We applied our model to the analysis of DnaK/DnaJ/GrpE-mediated refolding of luciferase[5] and
111 its variant LucDHis6[29]. Most of the relevant kinetic parameters for this bacterial Hsp70 system
112 have been carefully determined experimentally[33] (Table 1). Our model quantitatively reproduces
113 the experimentally observed refolding kinetics under various conditions, capturing the slow
114 spontaneous refolding and denaturation of luciferase, the acceleration of refolding with
115 chaperone assistance, and the necessity of GrpE (Fig. 2a, b). The refolding speed and yield reach

Table 1. The experimental kinetic parameters for the DnaK/DnaJ/GrpE chaperone system. All the parameters are determined at the temperature of 25 °C, except for the rate of conformational change of DnaK from closed to open conformations, which was measured at 15 °C, 25 °C, and 35 °C, yielding the parameters $k_C^{(0)}$ and E_a from a fitting of the Arrhenius equation to the measured rates at different temperatures.

Reaction	Parameter	Rate	Reference
$S + C \cdot ATP \rightleftharpoons S \cdot C \cdot ATP$	$k_{a,C\cdot ATP}^{(0)}$	$1.28 \times 10^6 \text{ M}^{-1} \cdot \text{s}^{-1}$	6
	$k_{d,C\cdot ATP}$	2.31 s^{-1}	6
$S + C \cdot ADP \rightleftharpoons S \cdot C \cdot ADP$	$k_{a,C\cdot ADP}^{(0)}$	$1.17 \times 10^4 \text{ M}^{-1} \cdot \text{s}^{-1}$	6
	$k_{d,C\cdot ADP}$	$9.1 \times 10^{-4} \text{ s}^{-1}$	6
$J + C \cdot ATP \rightleftharpoons J \cdot C \cdot ATP$	$k_{a,J\cdot C}$	$4.88 \times 10^4 \text{ M}^{-1} \cdot \text{s}^{-1}$	15 [a]
	$k_{d,J\cdot C}$	$1.6 \times 10^{-3} \text{ s}^{-1}$	46
$S \cdot C \cdot ATP \rightarrow S \cdot C \cdot ADP + Pi$	$k_h^{(0)}$	0.01 s^{-1}	15 [b]
$J \cdot S \cdot C \cdot ATP \rightarrow J \cdot S \cdot C \cdot ADP + Pi$	$k_h^{(J)}$	1.8 s^{-1} [c]	15
$C \cdot ADP \rightarrow C + ADP$	$k_{d,ADP}$	0.006 s^{-1}	47
$E + C \cdot ADP \rightleftharpoons E \cdot C \cdot ADP$	$k_{a,E\cdot C}$	$7.85 \times 10^6 \text{ M}^{-1} \cdot \text{s}^{-1}$	27 [d]
	$k_{d,E\cdot C}$	30 s^{-1}	27
$C_{\text{closed}} \cdot ATP \rightarrow C_{\text{open}} \cdot ATP$	$k_C^{(0)}$	$1.1 \times 10^{23} \text{ s}^{-1}$	45 [e]
	E_a/R	$17320 \text{ } K$	45

a. The association rate constant of DnaJ binding to DnaK was determined from the DnaJ concentration dependence of the DnaK ATP hydrolysis rates, by fitting the hydrolysis rate $k_h([J]) = K_h(1 + K_h)^{-1}k_h^{(J,\text{w/o S})} + (1 + K_h)^{-1}k_h^{(0,\text{w/o S})}$ where $K_h \equiv k_{a,J\cdot C} \cdot [J]/(k_{d,J\cdot C} + k_h^{(J,\text{w/o S})})$, to the experimental data with respect to $k_{a,J\cdot C}$, $k_h^{(J,\text{w/o S})}$, and $k_h^{(0,\text{w/o S})}$, yielding the $k_{a,J\cdot C}$ value in the table, $k_h^{(J,\text{w/o S})} = 0.76 \text{ s}^{-1}$, and $k_h^{(0,\text{w/o S})} = 6 \times 10^{-4} \text{ s}^{-1}$. We note that the hydrolysis rates are measured without a protein substrate (indicated by the superscript w/o S), which can further accelerate the hydrolysis. Surface plasmon resonance measurement of DnaJ binding to DnaK yielded $k_{a,J\cdot C} = 2.3 \times 10^4 \text{ M}^{-1} \cdot \text{s}^{-1}$ [46], in good agreement with our fit.

b. Substrate-free DnaK has a basal ATP hydrolysis rate of 0.001 s^{-1}, but the substrate can further accelerate ATP hydrolysis by up to 9-fold[15,48]. We take the ATP hydrolysis rate of substrate-bound DnaK to be 10-fold higher than the basal rate. The predictions of our model are insensitive to this parameter.

c. This is the experimental rate for the temperature $T = 25$ °C. For the higher temperature $T = 30$ °C, we used an arbitrary but reasonable 5.5-fold higher value of 10 s^{-1} because we could not find any reported experimental value for this temperature.

d. The kinetic rates for GrpE binding to DnaK were not determined, but the steady state ratio in the two-step dissociation reaction, $C \cdot ADP + E \rightleftharpoons E \cdot C \cdot ADP \rightleftharpoons E \cdot C + ADP$, $K_D' = (k_{d,E\cdot C} + k_{d,ADP})/k_{a,E\cdot C} = 20$ μM was determined. We chose an arbitrary diffusion limited association rate for GrpE binding to DnaK in our calculations.

e. We note that $k_C^{(0)}$ and E_a appear too large to be physically meaningful; they should instead be taken simply as numerical parameters that yield an excellent fit of the Arrhenius equation to the experimental data.

---

116 a maximum at the DnaK concentration of 1 μM, which is captured by our model (Fig. 2b, c). The
117 intermediate conformations U and F in our model may correspond to the experimentally
118 identified intermediate conformations I_2 and I_1 of luciferase[4]: the free energy difference between
119 N and F at 25 °C, according to the fitted parameters, is 20 kJ/mol, close to the experimental
120 value of 15 kJ/mol between N and I_1, measured at 10 °C. Consistent with previous experimental
121 observations[29], our model suggests that the Hsp70-accelerated refolding proceeds in two steps:
122 1) rapid unfolding of the misfolded substrate, stabilized by the ADP-bound DnaK, followed by
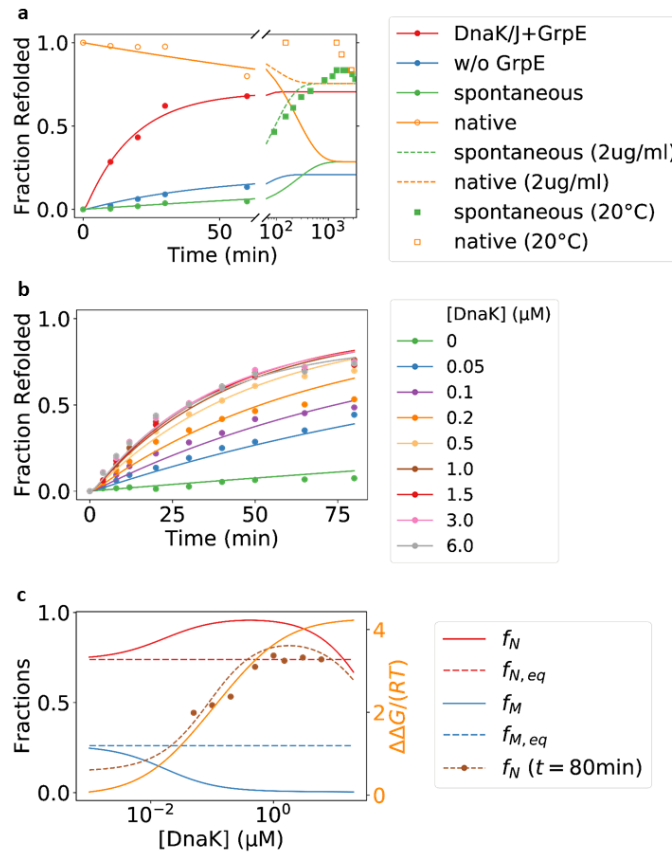123 2) slow conversion to the native state (Fig. 3a).

Figure 2. Our model is in good agreement with previous experimental studies of DnaK/DnaJ/GrpE-mediated refolding, and it predicts that DnaK and DnaJ cooperate to utilize the free energy of ATP hydrolysis to drive luciferase toward the native state. **a** The refolding of denatured luciferase under various conditions. The predictions of our model are shown in lines, whereas the experimental data are shown as filled circles[5]. The dashed lines show the spontaneous refolding and denaturation at the much lower substrate concentration of 0.032 μM (2 μg/ml), as in the corresponding experiments (empty circles and squares)[4]. The experiments of spontaneous refolding and denaturation were performed at 20 °C, lower than the temperature of 25 °C at which most of the kinetic parameters were obtained. In modeling the refolding, we assume that initially all the protein is in the misfolded/aggregated state, *i.e.*, $f_M (t = 0) = 1$; in modeling the denaturation, we assume that initially all the protein is in the native state, *i.e.*, $f_N (t = 0) = 1$. **b** The refolding of a luciferase mutant, LucDHis6[29], in the presence of DnaK at various concentrations. Although the experiments were performed at the slightly lower temperature of 22°C, the predictions of our model using the kinetic parameters derived for 25°C are nevertheless in quantitative agreement with the experimental data. **c** The native fraction ($f_N = [N] / [S]$, red) and the misfolded fraction ($f_M = [M] / [S]$, blue) of LucDHis6 at the steady state of DnaK-mediated refolding at various DnaK concentrations. The corresponding fractions in the chaperone-free folding equilibrium, $f_{N,eq}$ and $f_{M,eq}$, are shown as dashed lines. The unitless excess free energy $\Delta\Delta G / (RT)$ is shown in orange (right y-axis). The fractions after 80 min of refolding, starting from misfolded LucDHis6, are shown in brown. Our model is in good agreement with the experimental data (filled circles), and it suggests that the refolding is still incomplete even after 80 min. The fitting parameters in our model are given in Table 2, and the conditions of the experiments considered in this paper are summarized in Table 3.

124   At the steady state, the reactive flux along the ATP-driven cycle $U \rightarrow U \cdot C \cdot ATP \rightarrow$
125    $U \cdot C \cdot ADP \rightarrow F \cdot C \cdot ADP \rightarrow F \cdot C \cdot ATP \rightarrow F (\rightarrow U)$ (Fig. 3b) keeps the protein folding out of
126   equilibrium, elevating the native population above and suppressing the misfolded population
127   below their respective equilibrium values (Fig. 2c). The excess free energy at the steady state
128   always increases with increasing DnaK concentrations, but the native population reaches a

Table 2. The model parameters fit to the refolding experiments.

Reaction	Parameter	Luciferase		LucDHis6
		25 °C	**30 °C**	**22 °C**
$M \rightleftharpoons U$	$k_{M \rightarrow U}$ (s^{-1}) [a]	0.02	0.02	0.02
	$k_{U \rightarrow M}$ (M$^{-1} \cdot$ s^{-1})	9.4×10^8	3.4×10^9	6.4×10^7
$U \rightleftharpoons F$	$k_{U \rightarrow F}$ (s^{-1})	0.23	0.88	0.26
	$k_{F \rightarrow U}$ (s^{-1})	0.18	0.13	0.042
$F \rightleftharpoons N$	$k_{F \rightarrow N}$ (s^{-1}) [b]	5	5	5
	$k_{N \rightarrow F}$ ($10^{-3} \cdot$s^{-1})	1.4	20	1.1
$S + C \cdot X \rightleftharpoons S \cdot C \cdot X$	$n_C^{(U)}$	9.1	6.2	1.9
	$n_C^{(U)}/n_C^{(F)}$ [c]	20	20	20
$S + J \rightleftharpoons S \cdot J$	$K_{A,J}^{(U)}$ ($10^6 \cdot$ M^{-1})	13	22	54
$(J + C) \cdot S \rightleftharpoons (J \cdot C) \cdot S$	$[J]_{\text{eff}}$ (M) [d]	5×10^{-3}	5×10^{-3}	5×10^{-3}

a. The predictions of our model depend on the equilibrium constant $K_{M \rightleftharpoons U} = k_{M \rightarrow U}/k_{U \rightarrow M}$, but are degenerate with respect to the individual rates. We thus fix an arbitrary but plausible value for $k_{M \rightarrow U}$ and fit $k_{U \rightarrow M}$ to the experimental refolding data.

b. For the similar reason as above, we fix $k_{F \rightarrow N}$ and fit $k_{N \rightarrow F}$ to the refolding data.

c. There should be more accessible DnaK binding sites in the U state than in the F state. Here, we arbitrarily set the ratio between the two. Although the values of the other fitting parameters will change accordingly, the quality of the fit and the predictions of our model are insensitive to this ratio (at least for values between 1 and 100).

d. We assume that the effective distance, L, between the Hsp70 molecule and the J domain of the Hsp40 molecule bound to the same substrate molecule is $L = 4.3$ nm, the effective concentration is then $[J]_{\text{eff}} = N_A^{-1}/(L^3 4\pi/3) = 5 \times 10^{-3} M$. The quality of the fit and the predictions of our model are insensitive to this parameter.

129   maximum and then decreases (Fig. 2c), because at high DnaK concentrations, the substrate is
130   trapped in the DnaK-bound state and thus prevented from folding into the native state.

131   We used our model to estimate the ATP consumption in the DnaK/DnaJ/GrpE-mediated folding
132   of LucDHis6 (Fig. 4). In the initial minutes of refolding, approximately 150 ATP molecules are
133   consumed to refold one LucDHis6 (Fig. 4a), which is reasonably close to the experimental result
134   of ~50 ATP molecules consumed per refolded LucDHis6 when the stoichiometry of
135   DnaK:LucDHis6 is 1:1, significantly higher than the experimental number of ~5 when
136   LucDHis6 is in excess of DnaK, and significantly lower than the estimates of >1000 for many
137   other substrates in other experiments[29,34–36]. The discrepancy between the model and the
138   experimental results may be partially attributable to the approximations in our model and the
139   inaccuracies in the input kinetic parameters. ATP hydrolysis continues at the steady state and the
140   free energy is utilized to promote the native state and suppress the misfolded state (Fig. 4b, c).
141   As [DnaK] exceeds 1 µM, the ATP consumption rate increases rapidly without commensurate
142   increase in the excess free energy. Our analysis thus suggests that DnaK may be most free
143   energy efficient at maintaining protein folding out-of-equilibrium when its concentration is in the
144   sub-micromolar range, a prediction that may be tested experimentally.

145   Our model suggests that Hsp70 can keep a protein folded even if it thermodynamically favors
146   aggregation. The chaperone is thus able to play a critical role in maintaining protein
147   conformations, not just in the folding of nascent chains[37]. Higher DnaK concentrations are
148   required to suppress aggregation at increasing substrate concentrations (Fig. 5a) or at decreasing
149   substrate stabilities (Fig. 5b). This may explain how cells that overexpress DnaK can tolerate
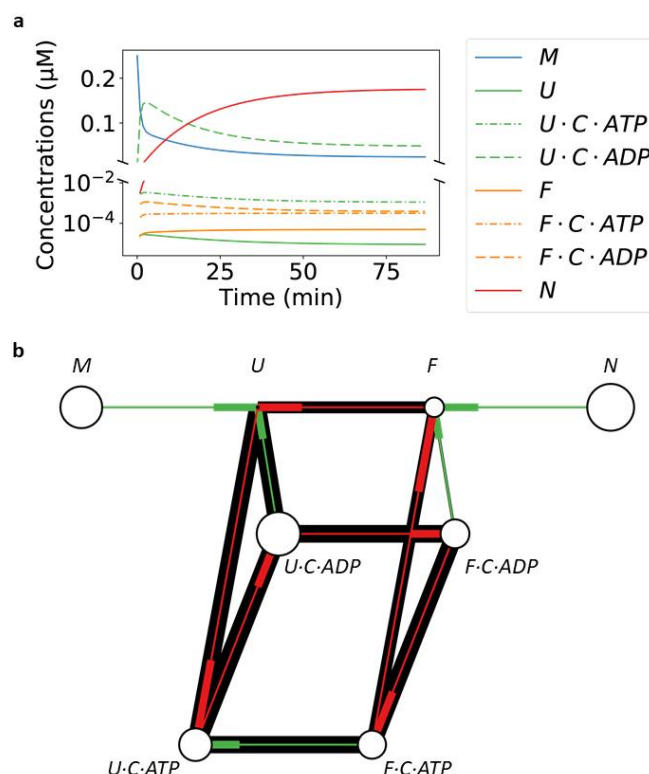150   higher numbers of mutations in the chaperone's substrates[38]. Because the excess free energy

Figure 3. The mechanism by which the Hsp70 chaperone system accelerates refolding and maintains the folding out of equilibrium. **a** The model prediction of the concentrations of different molecular species in DnaK/DnaJ/GrpE-mediated refolding of denatured luciferase. The substrate is primarily held by ADP-bound chaperone in the *U* state before slowly moving into the native state. **b** The reactive flux at the steady state. The thickness of each line is linear with respect to the logarithm of the absolute value of the reactive flux, and the thicker end of the thin, center line indicates the destination of the flux. The size of the circle at each node is linear with respect to the logarithm of the steady state fraction of the corresponding molecular species. The ATP-driven reaction cycle is highlighted in red.

151 plateaus at high chaperone concentrations (Fig. 2c), our results imply a limit on the
152 chaperones'capacity to prevent aggregation, in that there exists a threshold of aggregation
153 tendency (Fig. 5a, b, the black arrows) above which the chaperone can no longer maintain high
154 levels of native concentrations and prevent aggregation at the same time.

155 Our model suggests that Hsp70 only drives the folding of proteins with sufficiently slow
156 conversion between *U* and *F* states (Fig. 5c, d, e), implying that Hsp70 substrates tend to be slow
157 refolding proteins (Fig. 5d). If the conversion between *U* and *F* is too fast, the chaperone
158 diminishes, rather than increases, the native fraction in comparison to the chaperone-free
159 equilibrium. As the conversion slows, the chaperone drives the steady state native fraction
160 higher, but at the price of longer refolding time (Fig. 5e), a trade-off reminiscent of that between
161 speed and specificity in the kinetic proofreading mechanism[39,40], where the expenditure of free
162 energy (such as from ATP or GTP consumptions) is utilized to increase the specificity of
163 chemical reactions.

164 Our model explains the observation that folding is less efficient at both low and high DnaJ
165 concentrations[15] (Fig. 6a). At low DnaJ concentrations, ATP hydrolysis is slow, and nucleotide
166 exchange drives DnaK toward the ATP-state, in which it dissociates from the substrate rapidly
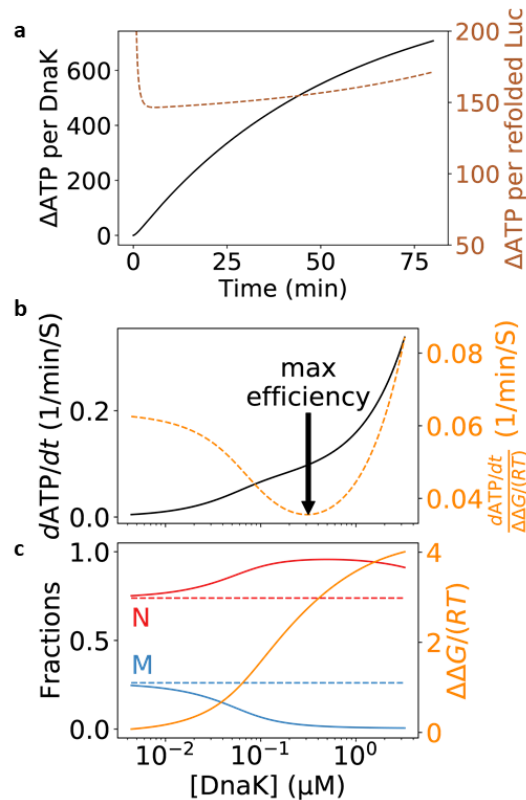167 and thus unable to prevent aggregation. At high DnaJ concentrations, a large fraction of the

Figure 4. Free energy consumption in DnaK/DnaJ/GrpE-mediated folding of LucDHis6. **a** ATP consumption in the course of refolding of denatured LucDHis6. The instantaneous rate of ATP consumption is given by $d\mathrm{ATP}/dt = \sum_{S\in\{U,F\}} k_h^{(S)}([J]) \cdot [S \cdot C \cdot ATP]$, and the number of hydrolyzed ATP per molecule of refolded substrate can be estimated by dividing the cumulative consumption, $\Delta\mathrm{ATP} = \int_0^\tau d\mathrm{ATP}$, by the number of refolded substrate molecules after time τ. Here, the DnaK concentration is 0.5 μM, and the other kinetic parameters are given in Table 1 and Table 2. The black curve shows the number of ATP molecules hydrolyzed per DnaK molecule after the given time. The brown curve shows the number of ATP molecules consumed per one molecule of refolded LucDHis6 (right y-axis) up to the given time, which increases to infinity at the steady state because no additional LucDHis6 is refolded, yet ATP hydrolysis continues. **b** and **c** ATP hydrolysis at the steady state. The ATP consumption rate per substrate, at various DnaK concentrations, is shown as the black curve in panel b, and the corresponding native (red) and misfolded (blue) fractions at the steady state are shown as solid lines in panel c. The native fraction is above and the misfolded fraction is below their respective equilibrium values (dashed flat lines). The excess free energy $\Delta\Delta G / (RT)$ is shown in orange (right y-axis) in panel c. We can measure the chaperones' free energy efficiency in maintaining the non-equilibrium by the ratio of the ATP consumption rate to the excess free energy at the steady state (orange, right y-axis, in panel b). The arrow indicates the DnaK concentration at which the chaperones utilize the least amount of ATP per unit of excess free energy.

168 substrate in the U state is bound to DnaJ. These DnaJ-bound substrate molecules are trapped in
169 the U state, unable to progress toward the F state, resulting in diminished folding.

170 Our model also explains the observation that folding decreases at both low and high GrpE
171 concentrations[27] (Fig. 6b). For the chaperone to effectively assist folding, nucleotide exchange
172 should be much slower than ATP hydrolysis when the chaperone binds to a substrate in the U
173 state, but much faster than ATP hydrolysis when it binds to a substrate in the F state, so that the
174 chaperone is driven toward the ADP-state in the former case, and toward the ATP-state in the
175 latter case (Fig. 1b). At low GrpE concentrations, nucleotide exchange is slow, leaving DnaK
176 bound to the substrate in the F state predominantly in the ADP-state—as reflected by the low
177 population of $F \cdot C \cdot ATP$ (Fig. 6b), slowing its dissociation from the substrate and thus
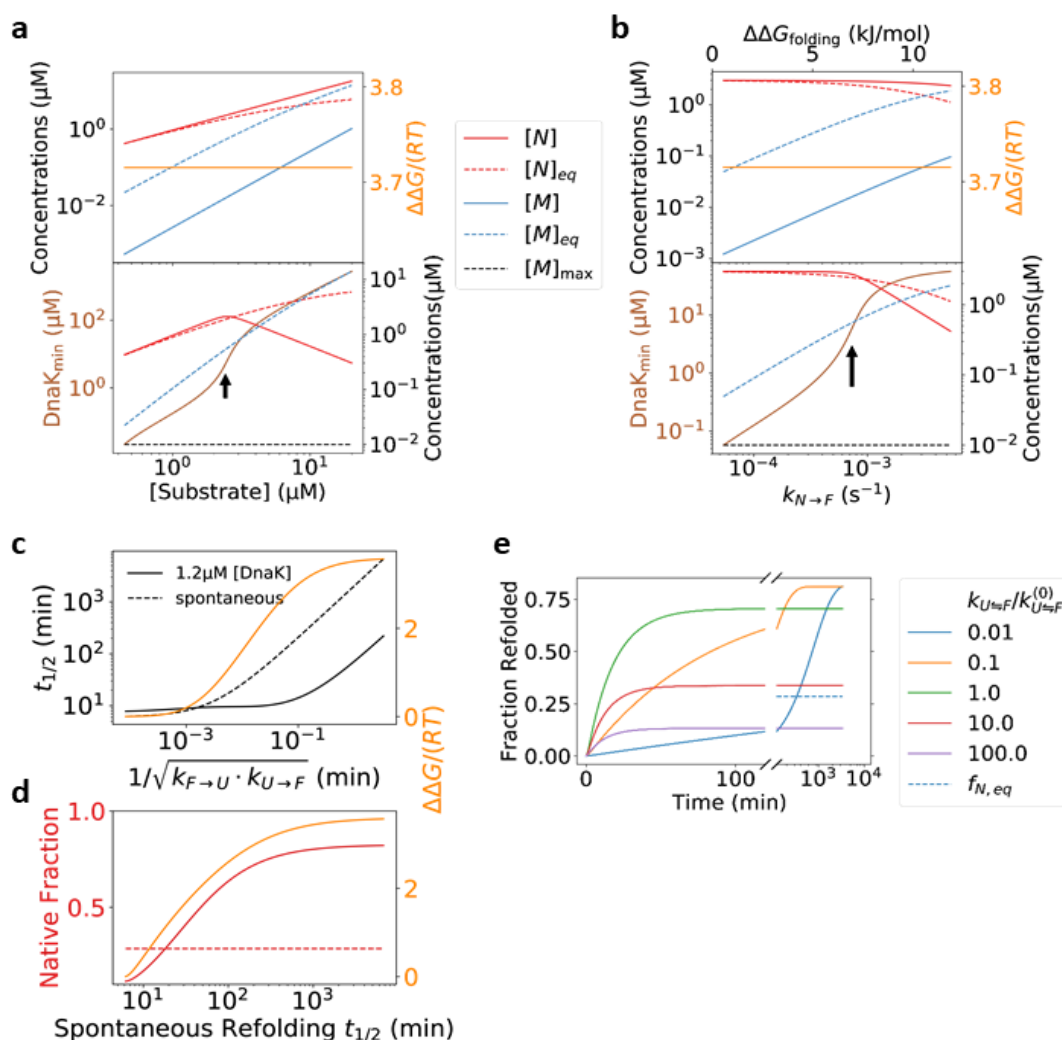
9

Figure 5. The capacity of the DnaK/DnaJ/GrpE chaperones to prevent aggregation and to elevate native protein concentrations. **a** The chaperones can prevent aggregation at increasing substrate concentrations. The rate of aggregation is taken to be proportional to the substrate concentration (see *Methods*). Top: the native and the misfolded steady state concentrations at increasing total LucDHis6 concentrations, with the DnaK concentration fixed at 1.2 μM. Bottom: the DnaK concentration required to maintain the misfolded protein concentration at or below $[M]_{max} = 0.01$ μM, as well as the steady state concentration of the native substrate at that DnaK concentration. **b** The chaperones can prevent aggregation at decreasing substrate stability. We vary the protein stability by changing the rate constant of conversion, $k_{N \to F}$, from the N state to the F state; the corresponding change in the folding free energy $\Delta\Delta G_{folding}$ is indicated on the top axis. The native and the misfolded concentrations, as well as the DnaK concentration required to prevent aggregation, are shown as in panel a. **c** and **d** Hsp70 is more efficient at folding substrates with slower conversion between the U and the F states. Here, we take the kinetic parameters of luciferase folding at 25 °C, and simultaneously scale the forward and reverse rates of the reaction $U \rightleftharpoons F$ by the same factor, thus changing the kinetics without affecting the folding equilibrium. The times, $t_{1/2}$, for the refolding of the misfolded substrate to reach half of the native fraction at equilibrium (spontaneous refolding) or the steady state (mediated by DnaK/DnaJ/GrpE), as well as the excess free energy (orange, right y-axis), are plotted against the hypothetic rates of conversion in c. The native fractions (red, left y-axis) and the excess free energy (orange, right y-axis) at the steady state are plotted against $t_{1/2}$ of spontaneous refolding in d; the equilibrium native fraction is shown as the red dotted line. **e** The time courses of Hsp70-mediated refolding of the misfolded substrate at different hypothetical rates of conversion between U and F (keeping $k_{U \to F}/k_{F \to U}$ constant). Higher steady state native fractions are obtained at the price of longer refolding times.
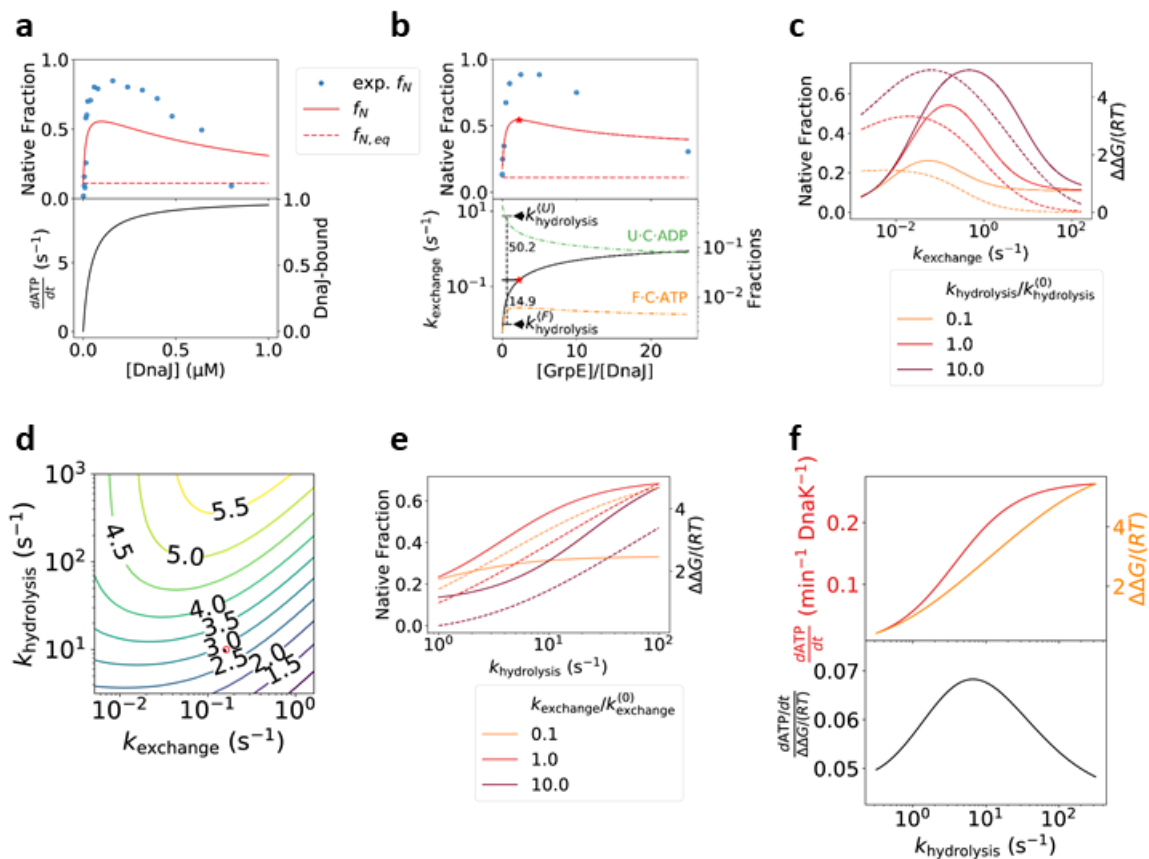
Figure 6. The rates of Hsp40-catalyzed ATP hydrolysis and NEF-catalyzed nucleotide exchange affect the efficiency of Hsp70-mediated folding. **a** Refolding of luciferase at various DnaJ concentrations. Top: the steady state native fractions predicted by our model, compared to the experimental data of refolding after 30 min at 30 °C [15]. Bottom: the ATP hydrolysis rate (left y-axis) and the fraction of substrate bound to DnaJ (right y-axis). **b** Refolding of luciferase at various GrpE concentrations. Top: the steady state native fractions predicted by our model, compared to the experimental data of refolding after 2 hours at 30 °C [27]. Bottom: the rate of nucleotide exchange at different GrpE concentrations (black line, left y-axis), and the populations of $F \cdot C \cdot ATP$ and $U \cdot C \cdot ADP$ (right y-axis). The optimal GrpE concentration is indicated by the red stars, and the in-plot numbers show the corresponding ratios of the nucleotide exchange rate to the ATP hydrolysis rates in the U and F states. In a and b, the rates of GrpE-catalyzed nucleotide exchange and DnaJ-catalyzed ATP hydrolysis are adjusted for the temperature of 30 °C (see *Methods* and Table 1). **c** Folding efficiency at different hypothetical rates of nucleotide exchange, for different values of the ATP hydrolysis rate in the U state. Native fractions (solid lines, left y-axis) are diminished at both low and high nucleotide exchange rates. At high rates of nucleotide exchange, the excess free energies (dashed lines, right y-axis) approach zero, indicating that Hsp70 can no longer drive protein folding. **d** The excess free energy as a function of the nucleotide exchange and the DnaJ-catalyzed ATP-hydrolysis rates. The rates used to model DnaK/DnaJ/GrpE-mediated folding at 30 °C are indicated by the red circle. **e** Folding efficiency increases with the DnaJ-catalyzed ATP hydrolysis rate, yielding higher native fractions (solid lines, left y-axis) and larger excessive free energies (dashed lines, right y-axis). **f** Higher ATP hydrolysis rate yields larger excess free energy (orange, right y-axis, top), at the price of higher rate of ATP consumption (red, left y-axis, top). The ratio of the two (bottom) changes only slightly.

178 preventing the latter from folding to the native state. At high GrpE concentrations, nucleotide
179 exchange is fast, and DnaK is driven into the ATP-state and does not stay bound to the substrate
180 in the U state long enough—as reflected by the decreasing population of $U \cdot C \cdot ADP$ (Fig. 6b)—
181 to prevent the substrate from aggregation. To maximize substrate folding, higher nucleotide
182 exchange rate should accompany higher stimulated ATP hydrolysis rate (Fig. 6c, d, e).

Table 3. The conditions of the refolding experiments (the corresponding references are in superscripts). **A**. Spontaneous refolding of guanidinium chloride (GdmCl)-denatured luciferase. **B**–**D**. DnaK/DnaJ/GrpE-mediated refolding of GdmCl-denatured luciferase. **E**. DnaK/DnaJ/GrpE-mediated refolding of LucDHis6 denatured by 4 freeze-thaw cycles. LucDHis6 is an engineered luciferase variant where the last 62 COOH-terminal residues are replaced by SKLSYEQDGLHAGSPAALEHHHHHH-COOH.

	A [4]	**B** [5]	**C** [15]	**D** [27]	**E** [29]
[DnaK] (μM)	0	1.25	0.8	0.8	0 to 6
[DnaJ] (μM)	0	0.25	0 to 0.8	0.16	0.3
[GrpE] (μM)	0	1.25	0.4	0 to 4	0.8
[S] (μM)	0.0324	0.25	0.08	0.08	3
[ATP] (mM)	0	1	5	N/A	5
[ADP] (mM)	0	0	0	N/A	0
T (°C)	20, 30	25	30	30	22

183 Our model predicts that Hsp70 chaperones with higher Hsp40-stimulated ATP hydrolysis rates
184 can drive substrate folding to higher native fractions (Fig. 6e), at the cost of higher free energy
185 expenditure (Fig. 6f). This result explains a previous experimental observation that a small
186 molecule that enhances ATP hydrolysis by Hsp40-bound Hsp70 can induce higher yields of
187 substrate folding[41]. Modulation of the ATP hydrolysis or the nucleotide exchange rates by small
188 molecules may represent a therapeutic opportunity in the treatment of misfolding- or
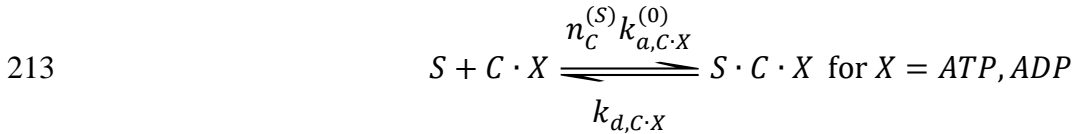189 proteostasis-related diseases[42].

190 **Discussion**

191 Our model makes two distinct predictions that subject it to future experimental tests and possible
192 falsification. First, it predicts that some thermodynamically unstable substrates depend on
193 continuous Hsp70 assistance to maintain their native structures, and such a substrate in the
194 steady state of Hsp70-mediated folding will gradually lose its native structure upon disruption of
195 the chaperone system. Second, it predicts that an Hsp70 molecule bound to a substrate molecule
196 will dissociate faster if subsequently the substrate molecule folds into the native state than if the
197 substrate molecule misfolds, and such a difference will vanish in the absence of Hsp40. The
198 second prediction may be tested by single molecule experiments[23,32], if, for instance, separate
199 fluorescence signals are available to detect Hsp70-substrate binding and substrate folding.

200 In support of the first prediction above, a recent experiment has demonstrated that luciferase at
201 37 °C can be kept active by the DnaK/DnaJ/GrpE chaperone system when there is sufficient
202 ATP, but it rapidly loses its activity when ATP is depleted by the addition of apyrase[11]. Here,
203 based on our model, we propose an alternative experiment, which avoids the complication that
204 apyrase also affects the luciferase assay: Hsp70-mediated maintenance of luciferase activity may
205 be disrupted by inhibiting the simultaneous binding of Hsp40 to Hsp70 and the substrate protein,
206 which can be implemented, for example, by adding a J-domain (e.g., DnaJ with its CTD deleted)
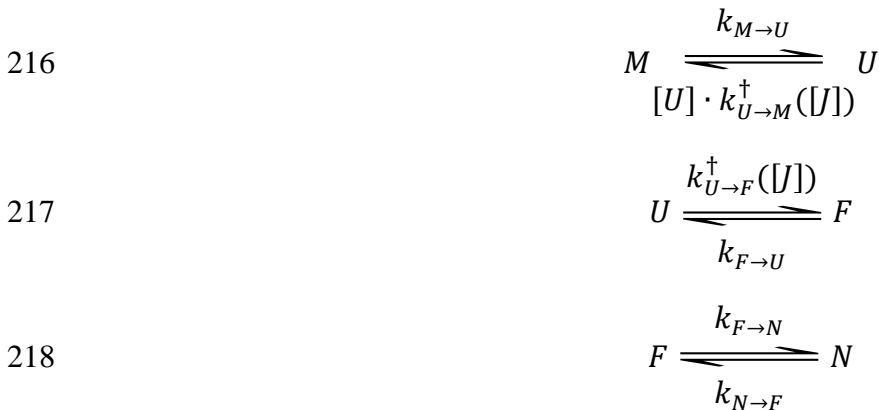207 in excess to the chaperone system.

Methods

Model of Hsp70-mediated protein folding. We denote Hsp70 as C, Hsp40 (J protein) as J, and the NEF as E. $[Y]$ denotes the solution concentration of the molecular species Y. There are four types of reactions explicitly considered in our model (Fig. 1b):
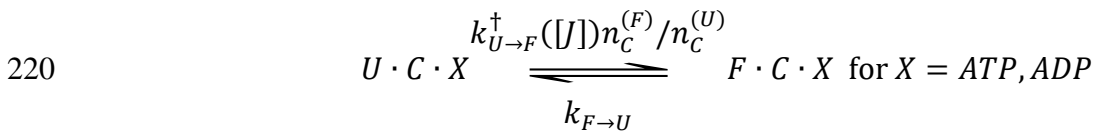
1) Hsp70 binding to the substrate.

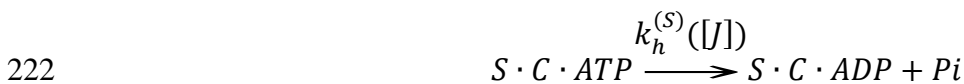$$S + C \cdot X \underset{k_{d,C \cdot X}}{\overset{n_C^{(S)} k_{a,C \cdot X}^{(0)}}{\rightleftharpoons}} S \cdot C \cdot X \text{ for } X = ATP, ADP$$

2) Conformational transitions of the substrate. An Hsp70-free substrate can adopt any of the four conformational states

$$M \underset{[U] \cdot k_{U \to M}^{\dagger}([J])}{\overset{k_{M \to U}}{\rightleftharpoons}} U$$

$$U \underset{k_{F \to U}}{\overset{k_{U \to F}^{\dagger}([J])}{\rightleftharpoons}} F$$

$$F \underset{k_{N \to F}}{\overset{k_{F \to N}}{\rightleftharpoons}} N$$

The chaperone-bound substrate can only be in and transition between the U and F states

$$U \cdot C \cdot X \underset{k_{F \to U}}{\overset{k_{U \to F}^{\dagger}([J]) n_C^{(F)}/n_C^{(U)}}{\rightleftharpoons}} F \cdot C \cdot X \text{ for } X = ATP, ADP$$

3) ATP hydrolysis.

$$S \cdot C \cdot ATP \xrightarrow{k_h^{(S)}([J])} S \cdot C \cdot ADP + Pi$$

4) Nucleotide exchange.

$$S \cdot C \cdot ADP + ATP \xrightarrow{k_e([E])} S \cdot C \cdot ATP + ADP$$

The details of the kinetic rates of the above reactions are described below.

Hsp70 binding to the substrate. The association rate constant of Hsp70 binding to a substrate in state S, $k_{a,C \cdot X}^{(S)}$, is determined by the number of accessible binding sites, $n_C^{(S)}$, in that conformation: $k_{a,C \cdot X}^{(S)} = n_C^{(S)} k_{a,C \cdot X}^{(0)}$, where $k_{a,C \cdot X}^{(0)}$ is the association rate constant of the chaperone binding to a fully accessible binding site, and $X = ATP, ADP$. The dissociation rate constant of

13

230   Hsp70 from the substrate, $k_{d,C \cdot X}$, does not depend on the substrate conformation, but depends on

231   whether nucleotide $X = ATP$ or ADP is bound. Experimentally, $k_{a,C \cdot ATP}^{(0)} \gg k_{a,C \cdot ADP}^{(0)}$ and

232     $k_{d,C \cdot ATP} \gg k_{d,C \cdot ADP}$. We assume $n_C^{(U)} > n_C^{(F)}$.

233   **Conformational transitions of the substrate**. The transition rates between conformations S and

234   S' are different between a chaperone-free substrate ($k_{S \to S'}$) and a chaperone-bound substrate

235   ($k_{S \cdot C \cdot X \to S' \cdot C \cdot X}$) (Fig. 1b). The condition of thermodynamic cycle closure dictates that

236

$$\frac{k_{S \cdot C \cdot X \to S' \cdot C \cdot X}}{k_{S' \cdot C \cdot X \to S \cdot C \cdot X}} = \frac{k_{a,C \cdot X}^{(S')}}{k_{a,C \cdot X}^{(S)}} \frac{k_{S \to S'}}{k_{S' \to S}} = \frac{n_C^{(S')}}{n_C^{(S)}} \frac{k_{S \to S'}}{k_{S' \to S}}.$$

237   Because Hsp40 has different affinities for different substrate conformations, the transition rates

238   between the conformations will depend on whether the substrate is bound to Hsp40. We treat the

239   effects of Hsp40 on the reactions implicitly by making the affected rate constants dependent on

240   the solution Hsp40 concentration $[J]$ (see below).

241   For the transition $U \cdot C \cdot X \rightleftharpoons F \cdot C \cdot X$, we assume that the bound chaperone does not hinder the

242   substrate to go from the F state to the U state, because a binding site available in the F state is

243   most likely also available in the U state (based on the assumption $n_C^{(U)} > n_C^{(F)}$). Thus we take

244     $k_{F \cdot C \cdot X \to U \cdot C \cdot X} = k_{F \to U}$. It follows from thermodynamic cycle closure that the rate of the reverse

245   transition—we use the superscript dagger to indicate that they are influenced by the presence of

246   Hsp40—is

247

$$k_{U \cdot C \cdot X \to F \cdot C \cdot X}^{\dagger}([J]) = k_{U \to F}^{\dagger}([J]) n_C^{(F)} / n_C^{(U)}$$

248   We take the rate of aggregation to be proportional to the substrate concentration:

249

$$k_{U \to M}([U], [J]) = [U] \cdot k_{U \to M}^{\dagger}([J])$$

250   The rates $k_{U \to S}^{\dagger}([J])$ (for $S = F, M$) depend on the affinities of Hsp40 for the substrate in different

251   conformational states. For simplicity, we assume that Hsp40 only binds to the substrate in the U

252   state, and consequently only the Hsp40-free substrate can change from conformation U to F or

253   M. The corresponding transition rates are

254

$$k_{U \to S}^{\dagger}([J]) \approx (1 - p_J([J])) \cdot k_{U \to S} \approx \frac{1}{1 + [J] \cdot K_{A,J}^{(U)}} k_{U \to S},$$

255   where $k_{U \to S}$ is the rate of transition $U \to S$ (for $S = F, M$) for an Hsp40-free substrate, p_J is the

256   probability that the substrate is Hsp40-bound, and $K_{A,J}^{(S)}$ is the binding constant of Hsp40 for the

257   conformational state S.

258   **Hsp40-substrate binding.** To keep our model simple, we do not explicitly consider the kinetics

259   of binding and unbinding between Hsp40 and the substrate, and make the approximation that

260   they are always at equilibrium. The key assumption of our model is that the fold-competent

261   conformation F is much less accessible to Hsp40 than the aggregation-prone conformation U,

262   i.e., $K_{A,J}^{(F)} \ll K_{A,J}^{(U)}$. To reduce the number of unknown parameters, we take $K_{A,J}^{(F)} \approx 0$, i.e., the

263   binding of Hsp40 to the fold-competent conformation is negligible, as in our derivation of the

264   transition rates above. We also neglect subtleties such as that the J domain may bind with

265 different affinities to Hsp70 in the ATP- and ADP-states[43]. The above approximations may
266 contribute to quantitative differences between the predictions of our model and the experimental
267 observations, particularly in predicting how folding changes with Hsp40 concentrations. The
268 binding and unbinding of Hsp40 to the substrate and to Hsp70 can be explicitly included in our
269 model at the cost of greater complexity and additional fitting parameters, but our simplified
270 treatment above is adequate for the key results in this work.

271 **ATP hydrolysis.** The Hsp40-stimulated Hsp70 ATP hydrolysis rate, $k_h^{(J)}$, can be orders-of-
272 magnitude higher than the unstimulated basal rate $k_h^{(0)}$. The ATP hydrolysis rate of Hsp70
273 bound to the substrate in the F state is simply $k_h^{(F)}([J]) = k_h^{(0)}$, following our approximation that
274 no Hsp40 binds to the substrate in the F state. When Hsp70 is bound to the substrate in the U
275 state, its average rate of ATP hydrolysis, given the solution Hsp40 concentration, $[J]$, can be
276 approximated by

277
$$k_h^{(U)}([J]) \approx p_J([J]) \left(\frac{K_h}{1+K_h} k_h^{(J)} + \frac{1}{1+K_h} k_h^{(0)} \right) + \left(1 - p_J([J]) \right) k_h^{(0)},$$

278 where $K_h \equiv k_{a,J\cdot C} \cdot [J]_{\text{eff}}/(k_{d,J\cdot C} + k_h^{(J)})$, with $k_{a,J\cdot C}$ and $k_{d,J\cdot C}$ being the association and
279 dissociation rates of J domain binding to Hsp70, and $[J]_{\text{eff}}$ being the effective concentration of a
280 substrate-bound Hsp40 molecule around an Hsp70 molecule bound to the same substrate
281 molecule. The first term on the right hand side is the steady state rate of catalysis, weighted by
282 the probability p_J that an Hsp40 is bound to the substrate and thus present to catalyze the
283 hydrolysis. Here we assume a high ATP concentration such that ATP binding to Hsp70 is fast
284 compared to other steps in ATP hydrolysis.

285 **NEF-catalyzed nucleotide exchange.** Because of the high concentration of ATP in cells and in
286 the refolding experiments, we treat this reaction as irreversible. The reaction proceeds in three
287 steps: 1) dissociation of ADP, 2) binding of ATP, and 3) conformational change of Hsp70 from
288 the closed conformation in the ADP-state to the open conformation in the ATP-state. The
289 conformational equilibrium between the open and closed conformations may be influenced by
290 Hsp40 binding to Hsp70[44], but this effect is not considered in our model for simplicity and lack
291 of experimental parameters. In absence of the nucleotide exchange factor, the rate limiting step
292 in the reaction is the dissociation of ADP, with the rate constant $k_{d,ADP}$, whereas when catalyzed
293 by the NEF, the rate limiting step is the conformational change, with rate constant k_C [27,45]. The
294 overall rate of reaction at a given NEF concentration, $[E]$, is then approximately

295
$$k_e([E]) = \frac{K_e}{1+K_e} k_C + \frac{1}{1+K_e} k_{d,ADP}$$

296 where $K_e \equiv k_{a,E\cdot C} \cdot [E]/(k_{d,E\cdot C} + k_C)$, with $k_{a,E\cdot C}$ and $k_{d,E\cdot C}$ being the association and dissociation
297 rates of NEF binding to Hsp70. The temperature dependence of k_C for DnaK has been
298 determined to satisfy the Arrhenius equation: $k_C(T) = k_C^{(0)} \exp(-E_a/(RT))$, where $R =$
299 8.314 J/mol/K is the gas constant.

300 **Solving the kinetic equations.** To simplify the calculations of refolding kinetics, we make the
301 approximation that the solution concentrations of Hsp70, Hsp40, and NEF remain constant
302 throughout the refolding process, which is true if they are in large excess of the substrate-bound
303 chaperone, cochaperone, and NEF. Under this approximation, refolding kinetics is described by
304 a set of linear ordinary differential equations, which are solved by the technique of eigenvalue
305 decomposition of the rate matrix. This simplification allows quick and robust fitting of the

15

306 folding kinetic parameters to the experimental refolding data. The steady state calculations do
307 not use this approximation.

Proof that without cochaperones Hsp70 cannot alter the population ratio between the
native and the misfolded states. Consider a hypothetical, single-conformation substrate s and a
reference reaction cycle of chaperone binding ($s + C \cdot X \rightleftharpoons s \cdot C \cdot X$ for $X = ATP, ADP$), ATP
hydrolysis ($s \cdot C \cdot ATP \rightarrow s \cdot C \cdot ADP + Pi$), and nucleotide exchange ($s \cdot C \cdot ADP + ATP \rightarrow$
$s \cdot C \cdot ATP + ADP$), where the ATP-bound and ADP-bound chaperones bind to s with the rate
constants $k_{a,C \cdot ATP}^{(0)}$ and $k_{a,C \cdot ADP}^{(0)}$, respectively. Let q, $q_{C \cdot ATP}$ and $q_{C \cdot ADP}$ be the fractions of the
hypothetical substrate that are chaperone-free (s), bound to an ATP-bound chaperone
($s \cdot C \cdot ATP$), and bound to an ADP-bound chaperone ($s \cdot C \cdot ADP$), respectively, at the steady
state of this reaction cycle. For the real substrate in Hsp70-mediated folding, let f_S and $f_{S \cdot C \cdot X}$
($X = ATP, ADP$) be the fractions of the free and the $C \cdot X$-bound substrates in conformation S,
and let $f_{S,eq}$ be the fraction of the substrate in conformation S at the folding equilibrium in the
absence of the chaperones. It can be verified that

$$f_S = Q^{-1} f_{S,eq} q$$

$$f_{S \cdot C \cdot X} = Q^{-1} f_{S,eq} n_C^{(S)} q_{C \cdot X}, \text{ for } X = ATP, ADP$$

where

$$Q = \sum_S f_{S,eq} \left(q + n_C^{(S)} (q_{C \cdot ATP} + q_{C \cdot ADP}) \right),$$

are the steady state solutions to the kinetic equations, given the condition of thermodynamic
cycle closure. Thus the ratio $f_S / f_{S'} = f_{S,eq} / f_{S',eq}$ is not altered by the chaperone, despite the
free energy expenditure of ATP hydrolysis. This holds true for all numbers of intermediate
states, so long as the ATP hydrolysis and the nucleotide exchange rates of the chaperone do not
depend on the conformational state of the bound substrate.

Author Contributions

HX designed and performed the research and wrote the paper.

References

1. Bukau, B., Weissman, J. & Horwich, A. Molecular chaperones and protein quality control. *Cell* **125,** 443–451 (2006).

2. Hartl, F. U., Bracher, A. & Hayer-Hartl, M. Molecular chaperones in protein folding and proteostasis. *Nature* **475,** 324–332 (2011).

3. Balchin, D., Hayer-Hartl, M. & Hartl, F. U. In vivo aspects of protein folding and quality control. *Science* **353,** aac4354 (2016).

4. Herbst, R., Schäfer, U. & Seckler, R. Equilibrium intermediates in the reversible

16

339   unfolding of firefly (Photinus pyralis) luciferase. *J. Biol. Chem.* **272,** 7099–7105 (1997).

340 5. Szabo, A., Langer, T., Schroder, H., Flanagan, J., Bukau, B. & Hartl, F. U. The ATP
341   hydrolysis-dependent reaction cycle of the Escherichia coli Hsp70 system DnaK, DnaJ,
342   and GrpE. *Proc. Natl. Acad. Sci.* **91,** 10345–10349 (1994).

343 6. Mayer, M. P., Schröder, H., Rüdiger, S., Paal, K., Laufen, T. & Bukau, B. Multistep
344   mechanism of substrate binding determines chaperone activity of Hsp70. *Nat. Struct. Biol.*
345   **7,** 586–593 (2000).

346 7. Mayer, M. P. Hsp70 chaperone dynamics and molecular mechanism. *Trends in*
347   *Biochemical Sciences* **38,** 507–514 (2013).

348 8. Barducci, A. & De Los Rios, P. Non-equilibrium conformational dynamics in the function
349   of molecular chaperones. *Current Opinion in Structural Biology* **30,** 161–169 (2015).

350 9. Goloubinoff, P. & Rios, P. D. L. The mechanism of Hsp70 chaperones: (entropic) pulling
351   the models together. *Trends in Biochemical Sciences* **32,** 372–380 (2007).

352 10. Santra, M., Farrell, D. W. & Dill, K. A. Bacterial proteostasis balances energy and
353   chaperone utilization efficiently. *Proc. Natl. Acad. Sci.* **114,** E2654–E2661 (2017).

354 11. Goloubinoff, P., Sassi, A. S., Fauvet, B., Barducci, A. & Rios, P. D. L. Chaperones
355   convert the energy from ATP into the nonequilibrium stabilization of native proteins. *Nat.*
356   *Chem. Biol.* **14,** 388–395 (2018).

357 12. Kampinga, H. H. & Craig, E. A. The HSP70 chaperone machinery: J proteins as drivers of
358   functional specificity. *Nature Reviews Molecular Cell Biology* **11,** 579–592 (2010).

359 13. Yang, J., Nune, M., Zong, Y., Zhou, L. & Liu, Q. Close and allosteric opening of the
360   polypeptide-binding site in a human Hsp70 chaperone BiP. *Structure* **23,** 2191–2203
361   (2015).

362 14. Kityk, R., Kopp, J., Sinning, I. & Mayer, M. P. Structure and dynamics of the ATP-bound
363   open conformation of Hsp70 chaperones. *Mol. Cell* **48,** 863–874 (2012).

364 15. Laufen, T., Mayer, M. P., Beisel, C., Klostermeier, D., Mogk, A., Reinstein, J. & Bukau,
365   B. Mechanism of regulation of Hsp70 chaperones by DnaJ cochaperones. *Proc. Natl.*
366   *Acad. Sci.* **96,** 5452–5457 (1999).

367 16. Alderson, T. R. R., Kim, J. H. H. & Markley, J. L. L. Dynamical structures of Hsp70 and
368   Hsp70-Hsp40 complexes. *Structure* **24,** 1014–1030 (2016).

369 17. Wittung-Stafshede, P., Guidry, J., Horne, B. E. & Landry, S. J. The J-Domain of Hsp40
370   couples ATP hydrolysis to substrate capture in Hsp70. *Biochemistry* **42,** 4937–4944
371   (2003).

372 18. Szabo, A., Korszun, R., Hartl, F. U. & Flanagan, J. A zinc finger-like domain of the
373   molecular chaperone DnaJ is involved in binding to denatured protein substrates. *EMBO*
374   *J.* **15,** 408–417 (1996).

375 19. Lu, Z. & Cyr, D. M. The conserved carboxyl terminus and Zinc finger-like domain of the
376   co-chaperone Ydj1 assist Hsp70 in protein folding. *J. Biol. Chem.* **273,** 5970–5978 (1998).

377 20. Perales-Calvo, J., Muga, A. & Moro, F. Role of DnaJ G/F-rich domain in conformational
378   recognition and binding of protein substrates. *J. Biol. Chem.* **285,** 34231–34239 (2010).

379 21. Rüdiger, S., Schneider-Mergener, J. & Bukau, B. Its substrate specificity characterizes the

380 DnaJ co-chaperone as a scanning factor for the DnaK chaperone. *EMBO J.* **20,** 1042–1050
381 (2001).

382 22. Sekhar, A., Velyvis, A., Zoltsman, G., Rosenzweig, R., Bouvignies, G. & Kay, L. E.
383 Conserved conformational selection mechanism of Hsp70 chaperone-substrate
384 interactions. *Elife* **7,** e32764 (2018).

385 23. Mashaghi, A., Bezrukavnikov, S., Minde, D. P., Wentink, A. S., Kityk, R., Zachmann-
386 Brand, B., Mayer, M. P., Kramer, G., Bukau, B. & Tans, S. J. Alternative modes of client
387 binding enable functional plasticity of Hsp70. *Nature* **539,** 448–451 (2016).

388 24. Ahmad, A., Bhattacharya, A., McDonald, R. A., Cordes, M., Ellington, B., Bertelsen, E.
389 B. & Zuiderweg, E. R. P. Heat shock protein 70 kDa chaperone/DnaJ cochaperone
390 complex employs an unusual dynamic interface. *Proc. Natl. Acad. Sci.* **108,** 18966–18971
391 (2011).

392 25. Han, W. & Christen, P. Mechanism of the targeting action of DnaJ in the DnaK molecular
393 chaperone system. *J. Biol. Chem.* **278,** 19038–19043 (2003).

394 26. Johnson, J. L. & Craig, E. A. An Essential Role for the Substrate-Binding Region of
395 Hsp40s in Saccharomyces cerevisiae. *J. Cell Biol.* **152,** 851–856 (2001).

396 27. Packschies, L., Theyssen, H., Buchberger, A., Bukau, B., Goody, R. S. & Reinstein, J.
397 GrpE accelerates nucleotide exchange of the molecular chaperone DnaK with an
398 associative displacement mechanism. *Biochemistry* **36,** 3417–3422 (1997).

399 28. Brehmer, D., Rüdiger, S., Gässler, C. S., Klostermeier, D., Packschies, L., Reinstein, J.,
400 Mayer, M. P. & Bukau, B. Tuning of chaperone activity of Hsp70 proteins by modulation
401 of nucleotide exchange. *Nat. Struct. Biol.* **8,** 427–432 (2001).

402 29. Sharma, S. K., Rios, P. D. L., Christen, P., Lustig, A. & Goloubinoff, P. The kinetic
403 parameters and energy cost of the Hsp70 chaperone as a polypeptide unfoldase. *Nat.*
404 *Chem. Biol.* **6,** 914–920 (2010).

405 30. Rios, P. D. L. & Barducci, A. Hsp70 chaperones are non-equilibrium machines that
406 achieve ultra-affinity by energy consumption. *Elife* **3,** e02218 (2014).

407 31. Astumian, R. D. Microscopic reversibility as the organizing principle of molecular
408 machines. *Nat. Nanotechnol.* **7,** 684–688 (2012).

409 32. Nunes, J. M., Mayer-Hartl, M., Hartl, F. U. & Müller, D. J. Action of the Hsp70
410 chaperone system observed with single proteins. *Nat. Commun.* **6,** 6307 (2015).

411 33. Hu, B., Mayer, M. P. & Tomita, M. Modeling Hsp70-mediated protein folding. *Biophys.*
412 *J.* **91,** 496–507 (2006).

413 34. Diamant, S., Peres Ben-Zvi, A., Bukau, B. & Goloubinoff, P. Size-dependent
414 disaggregation of stable protein aggregates by the DnaK chaperone machinery. *J. Biol.*
415 *Chem.* **275,** 21107–21113 (2000).

416 35. Diamant, S. & Goloubinoff, P. Temperature-controlled activity of DnaK-DnaJ-GrpE
417 chaperones: Protein-folding arrest and recovery during and after heat shock depends on
418 the substrate protein and the GrpE concentration. *Biochemistry* **37,** 9688–9694 (1998).

419 36. Goloubinoff, P., Mogk, A., Zvi, A. P. Ben, Tomoyasu, T. & Bukau, B. Sequential
420 mechanism of solubilization and refolding of stable protein aggregates by a bichaperone
421 network. *Proc. Natl. Acad. Sci.* **96,** 13732–13737 (1999).

422   37.   Calloni, G., Chen, T., Schermann, S. M., Chang, H., Genevaux, P., Agostini, F., Tartaglia,
423   G. G., Hayer-Hartl, M. & Hartl, F. U. DnaK functions as a central hub in the E. coli
424   chaperone network. *Cell Rep.* **1,** 251–264 (2012).

425   38.   Aguilar-Rodríguez, J., Sabater-Muñoz, B., Montagud-Martínez, R., Berlanga, V., Alvarez-
426   Ponce, D., Wagner, A. & Fares, M. A. The molecular chaperone DnaK is a source of
427   mutational robustness. *Genome Biol. Evol.* **8,** 2979–2991 (2016).

428   39.   Murugan, A., Huse, D. A. & Leibler, S. Speed, dissipation, and error in kinetic
429   proofreading. *Proc. Natl. Acad. Sci.* **109,** 12034–12039 (2012).

430   40.   Hopfield, J. J. Kinetic Proofreading: A New Mechanism for Reducing Errors in
431   Biosynthetic Processes Requiring High Specificity. *Proc. Natl. Acad. Sci.* **71,** 4135–4139
432   (1974).

433   41.   Wisén, S., Bertelsen, E. B., Thompson, A. D., Patury, S., Ung, P., Chang, L., Evans, C.
434   G., Walter, G. M., Wipf, P., Carlson, H. A., Brodsky, J. L., Zuiderweg, E. R. P. &
435   Gestwicki, J. E. Binding of a small molecule at a protein-protein interface regulates the
436   chaperone activity of Hsp70-Hsp40. *ACS Chem. Biol.* **5,** 611–622 (2010).

437   42.   Labbadia, J. & Morimoto, R. I. The Biology of proteostasis in aging and disease. *Annu.*
438   *Rev. Biochem.* **84,** 435–464 (2015).

439   43.   Kim, J. H., Alderson, T. R., Frederick, R. O. & Markley, J. L. Nucleotide-dependent
440   interactions within a specialized Hsp70/Hsp40 complex involved in Fe–S cluster
441   biogenesis. *J. Am. Chem. Soc.* **136,** 11586–11589 (2014).

442   44.   Yang, J., Zong, Y., Su, J., Li, H., Zhu, H., Columbus, L., Zhou, L. & Liu, Q.
443   Conformation transitions of the polypeptide-binding pocket support an active substrate
444   release from Hsp70s. *Nat. Commun.* **8,** s41467-17 (2017).

445   45.   Slepenkov, S. V & Witt, S. N. Kinetics of the reactions of the Escherichia coli molecular
446   chaperone DnaK with ATP: evidence that a three-step reaction precedes ATP hydrolysis.
447   *Biochemistry* **37,** 1015–1024 (1998).

448   46.   Suh, W.-C., Burkholder, W. F., Lu, C. Z., Zhao, X., Gottesman, M. E. & Gross, C. A.
449   Interaction of the Hsp70 molecular chaperone, DnaK, with its cochaperone DnaJ. *Proc.*
450   *Natl. Acad. Sci.* **95,** 15223–15228 (1998).

451   47.   Russell, R., Jordan, R. & McMacken, R. Kinetic characterization of the ATPase cycle of
452   the DnaK molecular chaperone. *Biochemistry* **37,** 596–607 (1998).

453   48.   McCarty, J. S., Buchberger, A., Reinstein, J. & Bukau, B. The role of ATP in the
454   functional cycle of the DnaK chaperone system. *J. Mol. Biol.* **249,** 126–137 (1995).